ACS APPLIED MATERIALS & INTERFACES

Letter

www.acsami.org

Superhydrophobic Porous Surfaces: Dissolved Oxygen Sensing

Yu Gao, Tao Chen, Shunsuke Yamamoto, Tokuji Miyashita, and Masaya Mitsuishi*

Institute of Multidisciplinary Research for Advanced Materials, Tohoku University, 2-1-1 Katahira, Aoba-ku, Sendai 980-8577, Japan

Supporting Information

ABSTRACT: Porous polymer films are necessary for dissolved gas sensor applications that combine high sensitivity with selectivity. This report describes a greatly enhanced dissolved oxygen sensor system consisting of amphiphilic acrylamide-based polymers: poly(*N*-(1H, 1H-pentadecafluorooctyl)-methacrylamide) (pC7F15MAA) and poly(*N*-dodecylacrylamide-*co*-5- [4-(2-methacryloyloxyethoxy-carbonyl)phenyl]-10,15,20-triphenylporphinato platinum(II)) (p(DDA/PtTPP)). The nanoparticle formation capability ensures both superhydrophobicity with a water contact angle greater than 160° and gas permeability so that molecular oxygen enters the film from water. The film was prepared by casting a mixed solution of pC7F15MAA and p(DDA/PtTPP) with AK-225 and acetic acid onto a solid substrate. The film has a porous structure comprising nanoparticle assemblies with diameters of several hundred nanometers. The film shows exceptional performance as the oxygen sensitivity reaches 126: the intensity ratio at two oxygen concentrations (I_0/I_{40}) respectively corresponding to dissolved oxygen concentration 0 and 40 (mg L^{-1}). Understanding and controlling porous nanostructures are expected to provide opportunities for making selective penetration/separation of molecules occurring at the superhydrophobic surface.

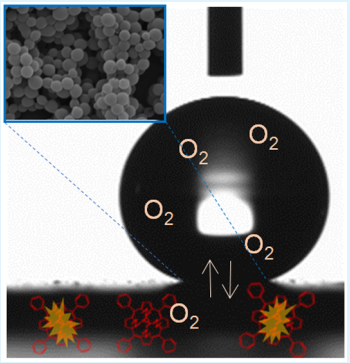

KEYWORDS: *amphiphilic, fluorinated polymer, nanoparticle, porphyrin, phosphorescence*

Superhydrophobic surfaces, with a water contact angle apparently greater than 150°, have attracted much attention because of their unique surface properties:[1] they are self-cleaning, water repellant, superamphiphobic,[2] superomniphobic,[3] and useful for water collection.[4] Their surfaces offer a unique confined space: gas−liquid−solid triple point. The liquid, water, is separated by a horizontal line. Underneath the interface, the air phase is maintained on a nanometer scale once the liquid is touched on the surface. The surface porosity serves as a reservoir to entrap gas. Theoretically, the surface is well-described by the so-called Cassie−Baxter Law,[5] but very little attention has been devoted to how the biphasic surface, one of which is air, brings about selective transport between different phases.[6−8]

In terms of the selective permeability, fluorinated polymers serve as promising materials because of their good water repellency and their low permeability to water. Compared with hydrocarbon polymer materials, they have higher oxygen gas permeability.[9] Considering their impermeability to water, surface wettability control, i.e., superhydrophobic states,[10] will help enhance selective permeability: the air (oxygen) can cross bidirectionally through the interface. However, the liquid (water) cannot pass through the composite surface. Such a critical condition offers selective transport of the gas from the solution.[7]

Highly sensitive detection of dissolved oxygen in water has been investigated intensively because of a demanding variety of purposes including biological,[11] industrial,[12] and environmental[13] monitoring, and medical applications.[14] In terms of commercially available sensor systems for oxygen detection, most detection systems are based on electron or light signals: electrochemistry,[15] fluorescence, and phosphorescence. Light transducer systems are preferred because some targets are highly explosive, such as redoxactive targets. Herein, we demonstrate enhanced oxygen sensor capability in water. Results show that amphiphilic fluorinated polymer enables facile superhydrophobic surface formation merely by spreading its solution on a solid substrate. The film has a porous nature created by the nanoparticle assemblies with several hundred nanometer diameters. The luminescence intensity ratio at the dissolved oxygen concentrations of 0 and 40 mg L^{-1} in water reached 126, which is the highest value reported to date. The technique presents a new field of analytical and sensor science at the interface of different phases.

Fluorinated amphiphilic polymer, poly(*N*-1H, 1H-pentadecafluorooctyl methacrylamide) (pC7F15MAA, Figure 1a) is soluble in AK-225, but insoluble in other solvents (chloroform, THF, acetone, acetic acid, water).[16] The specific feature of pC7F15MAA is that the polymer has good amphiphilic properties leading to an ultrathin monolayer formation at the air−water interface. Dropcasting the mixed solution of two polymers on solid substrates with two miscible but opposite solvents, AK-225 and acetic acid, we prepared a pC7F15MAA film with 5 wt % p(DDA/PtTPP) (Figure 1a), which shows a reflective white-color (Figure 1b).[17] Scanning electron microscopy revealed that the film comprises nanoparticles with 100−500 nm diameter (Figure 1c). The size and the film thickness (approximately 2 μm) were controllable by adjusting

Received: December 29, 2014
Accepted: February 4, 2015
Published: February 9, 2015

DOI: 10.1021/am509147h
ACS Appl. Mater. Interfaces 2015, 7, 3468−3472

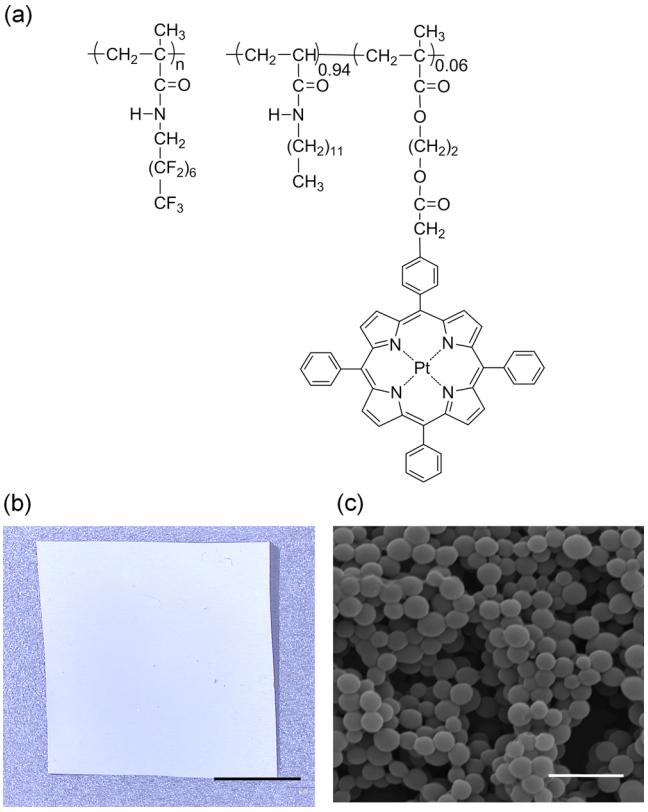

Figure 1. (a) Chemical structures of pC7F15MAA and p(DDA/PtTPP), (b) photograph of pC7F15MAA/p(DDA/PtTPP) mixed film on a silicon wafer (scale bar = 2 mm). (c) Scanning electron microscopy image of the film (scale bar = 2 μm).

the mixing ratio of solvents and total concentration. We also confirmed that p(DDA/PtTPP) alone cannot form nanoparticles. Also, low-molecular-weight compounds such as PtOEP form crystallines that are separated from pC7F15MAA nanoparticles. Work related to the relation between polymer design and nanoparticle formation is in progress.

Despite the facile preparation method, the results are remarkable. The water droplet contact angle on the film exceeded 150° with low hysteresis (<2°), which proves that the film has a superhydrophobic character (162° in Figure 2a). The critical surface energy of the superhydrophobic surface was ascertained as 18.7 mN m^{-1} (Figure 2b, see Figure S1 in the Supporting Information for comparison), indicating that the surface is occupied by CF_2 and CF_3 groups.[18] That is, the pC7F15MAA side chains are oriented in the outward direction of the nanoparticle surface. A selected time sequence of snapshots illustrates clearly that a water droplet, even with 20 μL volume, can bounce freely on the pC7F15MAA/p(DDA/PtTPP) film (Figure 3c); a dimensionless Weber number (*We*) was *We* = 17. The impact and after-impact velocities were also calculated as 0.85 (ms^{-1}) and 0.68 (ms^{-1}); the restitution coefficient remains high as about 0.8, even at a large Weber number. This finding suggests good water-repellent properties of pC7F15MAA/p(DDA/PtTPP) film.

Angle-dependent XPS measurements elucidate the chemical composition and the depth profile of the porous film. Figure 3a shows the C 1s XPS spectra of pC7F15MAA/p(DDA/PtTPP) film monitored varying a takeoff angle from 15° to 75°. The data reflect the information related to the chemical components 2 nm to approximately 10 nm far from the top surface of the

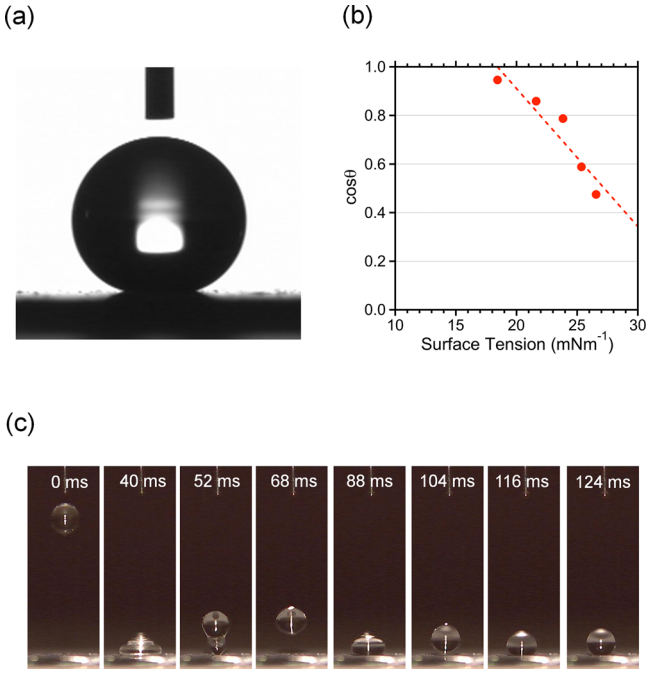

Figure 2. (a) Water contact angle on the pC7F15MAA/p(DDA/PtTPP) film. (b) Zisman plot of the pC7F15MAA/p(DDA/PtTPP) film. (c) Photographs of the water droplet (20 μL) bounced on the pC7F15MAA/p(DDA/PtTPP) film.

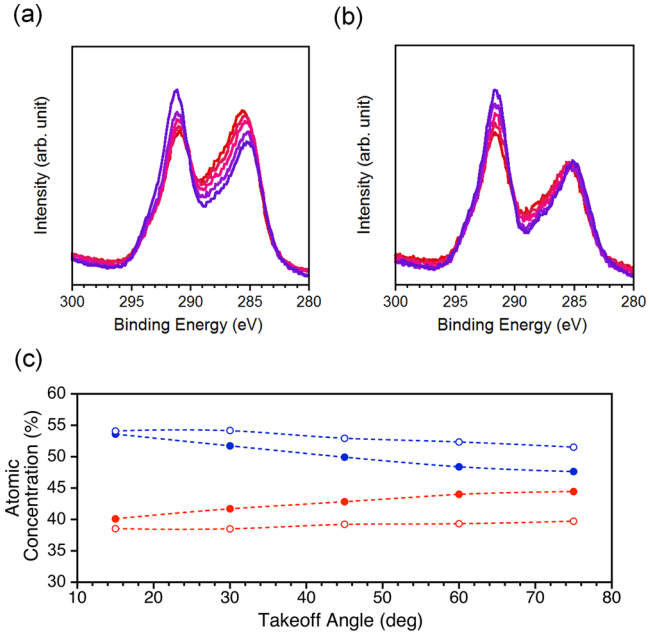

Figure 3. (a) Angle-resolved XPS spectra of (a) pC7F15MAA/p(DDA/PtTPP) film and (b) pC7F15MAA film. (c) Atomic concentration (fluoride (blue) and carbon (red)) of pC7F15MAA/p(DDA/PtTPP) film (filled circle) and pC7F15MAA film (open circle) as a function of the takeoff angle.

film.[19] The spectra in Figure 3a show two peaks: 285.2 and 291.3 eV. These peaks are ascribed to −C−C and $-CF_2$ atoms.[20] The shoulder at 293.4 eV is related with $-CF_3$ atoms, reflecting that the nanoparticle surface is to a larger degree covered with CF_3 groups. Apparently, the C atom concentration increases but the F atom concentration decreases in the pC7F15MAA/p(DDA/PtTPP) film (Figure 3a) as the

DOI: 10.1021/am509147h
ACS Appl. Mater. Interfaces 2015, 7, 3468−3472

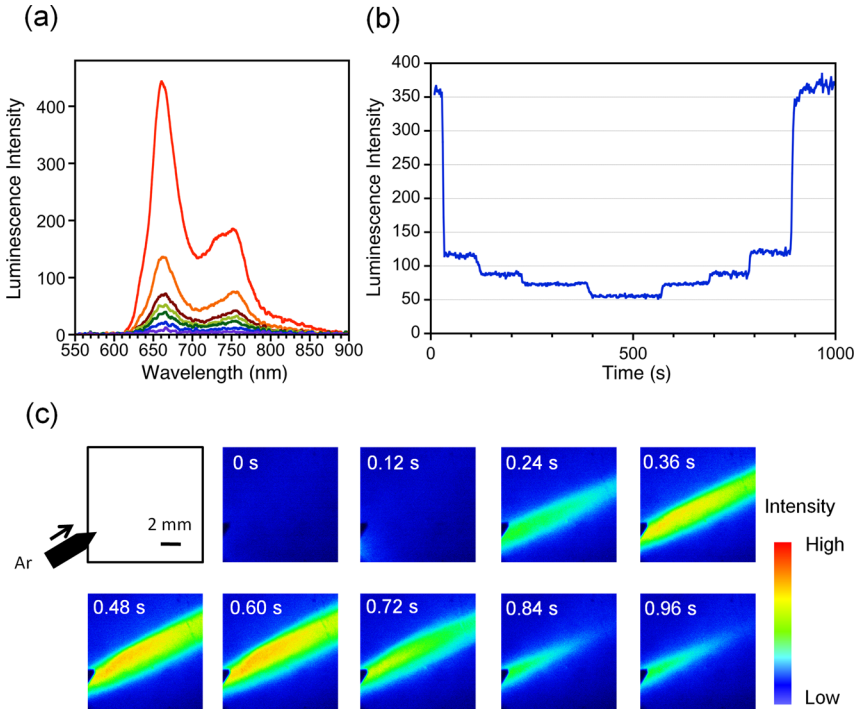

Figure 4. (a) Luminescence spectra of the pC7F15MAA/p(DDA/PtTPP) film in gas phase. The oxygen concentration was changed from 0%−100% (0 (red), 2 (orange), 6 (brown), 9 (lime green), 14 (green), 33 (blue), and 100% (purple) from the top). The excitation wavelength was 441.6 nm. (b) Time course of the luminescence intensity as a function of oxygen concentration. (c) Microscopic luminescence image for argon gas flow. A schematic of the experimental setup is shown at the top left. The values correspond to time (s).

takeoff angle increases, although no remarkable change is observed at 285.2 eV for the pC7F15MAA film (Figure 3b). The atomic concentration of the film at a takeoff angle of 15° is almost equal to that of pC7F15MAA film (Figure 3c). That is to say, the chemical composition of the outermost surface of pC7F15MAA/p(DDA/PtTPP) film is identical to that of single pC7F15MAA film. The increase (C atom concentration) and the decrease (F atom concentration) at higher takeoff angles indicate that p(DDA/PtTPP) is located close to the nanoparticle surface. Consequently, we infer that the top surface of the nanoparticles is occupied by fluorinated components. Therefore, the p(DDA/PtTPP) component is embedded in pC7F15MAA. The resulting porous film exhibits a superhydrophobic surface.

Platinum(II) porphyrins have strong luminescence (phosphorescence) at the red wavelength region. The luminescence intensity is well-known to depend on the surrounding oxygen concentration.[9,12] The pC7F15MAA/p(DDA/PtTPP) film provides surface light scattering (Figure 1b), which enhances the luminescence emission received by the detector. With the porphyrin chromophores closely packed and located close to the nanoparticle surface, analysis of oxygen information is fast and sensitive. The porous film exhibits good oxygen sensitivity in gas phase (Figure 4a). The film was placed in an in-house cuvette; the oxygen concentration was regulated by a portable gas mixture device. The luminescence intensity at 660 nm decreased drastically as the oxygen concentration increased. The film also has good reversibility for the oxygen concentration (Figure 4b). As shown in the Stern−Volmer plot (Figure S2 in the Supporting Information), the film exhibits a good linear relation between the oxygen concentration and the intensity ratio (I_0/I). However, the sensitivity value (I_0/I_{100}) was not so much higher than that described in our previous report.[21] In terms of the oxygen sensitivity, the film thickness (5 μm) as well as the nanoparticle structure in which p(DDA/PtTPP) is embedded inside the film might affect the luminescence behavior. The time response was determined to be 0.9 and 0.5 s, when switching from Ar to air atmosphere or vice versa (Figure S3 in the Supporting Information). These values, compared with those of previous reports, underscore the excellent performance of our sensor system.[22] It is noteworthy that the uniform coating of the porous pC7F15MAA/p(DDA/PtTPP) film enables clear mapping with microscopic scale. Figure 4c shows time-resolved microscopic luminescence images of the pC7F15MAA/p(DDA/PtTPP) film. Argon gas flow is given on the surface through a needle from the bottom left corner at 0 s. The gas value is closed at 0.60 s. Changes in the argon gas flow are viewed clearly as luminescence images in a millisecond time range.

The salient benefits of the superhydrophobic and porous pC7F15MAA/p(DDA/PtTPP) film are the following: (1) the surface is well described with the Cassie−Baxter model in which the surface is classified with two components, i.e., air and the solid included fluorinated components; and (2) higher diffusion of molecular oxygen in the porous space than in liquid, although water is repelled at the superhydrophobic surface and is entrapped at the interface, which engender highly sensitive detection of oxygen in water. The oxygen passing through the interface consequently encounters the porphyrin in the film. Figure 5a portrays luminescence spectra of the pC7F15MAA/p(DDA/PtTPP) film as a function of dissolved oxygen concentration. We set the film in the quartz cell filled with water. Measurements were conducted after bubbling the water at a certain oxygen concentration for at least 10 min. The luminescence intensity decreased drastically as the oxygen concentration increased. The linear relation in the Stern−

DOI: 10.1021/am509147h
ACS Appl. Mater. Interfaces 2015, 7, 3468−3472

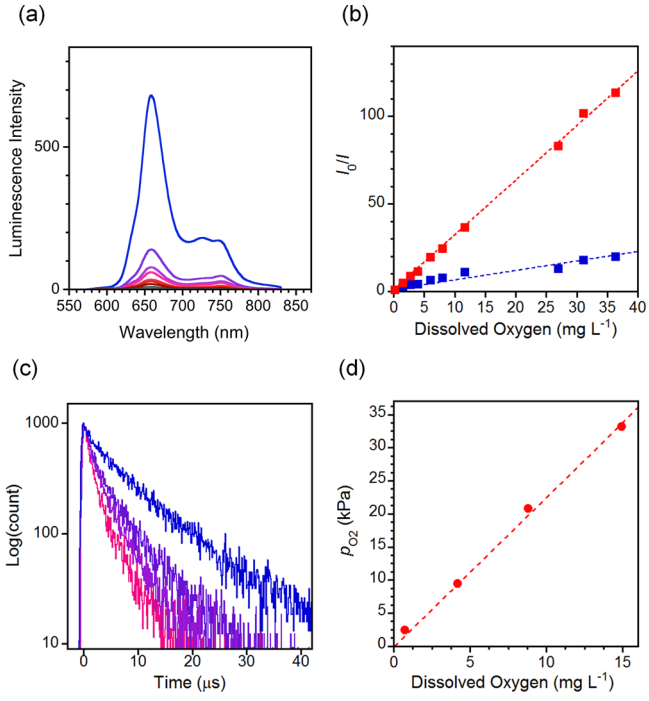

Figure 5. (a) Luminescence spectra of a porous pC7F15MAA/p(DDA/PtTPP) film in water as a function of oxygen concentration in the range of 0.1 (mg L^{-1}) (top) to 40 (mg L^{-1}) (bottom). (b) Stern–Volmer plots for the porous film (red) and the cast film (c) Time-resolved luminescence decay curves for pC7F15MAA/p(DDA/PtTPP) film in water: (from the top) 0.7, 4.2, 8.8, and 15.0 mg L^{-1} oxygen concentration. (d) Partial oxygen pressure in pC7F15MAA/p(DDA/PtTPP) films as a function of the dissolved oxygen concentration.

Volmer plot is maintained at 0–40 mg L^{-1} (Figure 5b). The sensitivity (I_0/I_{40}) reaches 126, which is the highest value reported to date.[23] For comparison, a Stern–Volmer plot of a pC7F15MAA/p(DDA/PtTPP) film cast with AK-225 alone is shown in Figure 5(b) (blue curve). The film exhibits no nanoparticle formation (Figure S4 in the Supporting Information); the water contact angle was 106°. The cast film (blue) yielded lower sensitivity (I_0/I_{40} = 22.6). Results imply that the porous structure is extremely effective at enhancing the dissolved oxygen sensitivity.

Deeper understanding of the pC7F15MAA/p(DDA/PtTPP) film structure enables us to elucidate how the dissolved oxygen behaves in the porous film. A superhydrophobic surface consists of two components: a water contact region and an air region. The air–liquid interface fraction of the pC7F15MAA/p(DDA/PtTPP) film underneath the water droplet was determined as 93%. Subsequently, QCM measurements revealed that the porous film had 74% porosity (see Supporting Information). Results imply that the void serves as "an external lung" to exchange the dissolved oxygen with the surrounding water.[24] We also monitored the luminescence decay curves of the film in water by varying the dissolved oxygen concentration (Figure 5c). Luminescent decay data were obtained using a streak scope system with a Q-switched Nd:YAG laser (5 ns, 10 Hz, 355 nm). All luminescence decayed single exponentially. The decay curves were fit with a single exponential function. We also monitored how the lifetime is related with the partial pressure of oxygen in gas phase using a pressure-controlled chamber that was produced in-house. The lifetime in the gas phase is well described by an empirical equation (Figure S5 in the Supporting Information). The control experiment enables determination of the partial pressure of oxygen in the pC7F15MAA/p(DDA/PtTPP) film once we obtain information related to the lifetime even in water. A linear relation is clear between the partial pressure of oxygen in gas phase and the dissolved oxygen concentration (Figure 5d). The line in Figure 5d is drawn using Henry's Law.

$$p_{O_2} = HC \quad (1)$$

Therein, p_{O_2} represents the partial pressure of oxygen in the gas phase, H stands for the Henry's Law constant, and C signifies the dissolved oxygen concentration in water. We used the Henry's Law constant for oxygen at 20 °C (2.27 (kPa L mg^{-1})).[25] The complete agreement constitutes strong evidence that the void of the film is occupied by gas phase. Furthermore, the lifetime at 20 kPa (2.5 μs) is equal to that at ambient dissolved oxygen concentration (8.8 mg L^{-1}). These results suggest that the equilibrium state is maintained between the entrapped gas and dissolved oxygen through the superhydrophobic surface of the pC7F15MAA/p(DDA/PtTPP) film. Enhancement of the sensitivity in water, when compared between Figure S2 in the Supporting Information and Figure 5b, might reflect less light scattering in water than in gas phase. Regarding the film time response, it lies on the order of 1×10^2 s (Figure S6 in the Supporting Information), which is not surprising. Generally, approximately 1 min is necessary to reach equilibrium across the air–liquid interface. In that sense, the present sensor system offers good time response as well as high sensitivity for dissolved oxygen.

In conclusion, we demonstrated a new sensing system for dissolved oxygen detection based on surface wettability and oxygen sensitive luminescence. A superhydrophobic surface was realized using a facile bottom-up approach: casting a mixed solution of two amphiphilic polymers, pC7F15MAA and p(DDA/PtTPP) on solid substrates. A white opaque and porous film was obtained, which consisted of nanoparticles of 100–500 nm diameter. Because of the good oxygen permeability and low surface tension of fluorinated side chains, oxygen detection was demonstrated in both air and water. The film provides especially excellent oxygen sensitivity in water (I_0/I_{40} = 126), which is the highest value reported to date.[23] The diameter of molecular oxygen is 0.3 nm, resulting in the mean free path 100 nm at room temperature and ambient pressure.[26] The path length is comparable to the size of porosity: Oxygen molecules can move more freely in the porous film. For that reason, our porous film shows the highest sensitivity for detecting dissolved oxygen. The free volume of conventional cast films is in the single-nanometer range. Molecular oxygen moves less freely, even if it comes across the water–film interface, leading to luminescence quenching restrained at the film surface. Much work remains to elucidate nanoparticle permeability and structure.

■ ASSOCIATED CONTENT

Supporting Information

Materials, experimental details, and supplemental figures. This material is available free of charge via the Internet at http://pubs.acs.org/.

DOI: 10.1021/am509147h
ACS Appl. Mater. Interfaces 2015, 7, 3468–3472

AUTHOR INFORMATION

Corresponding Author

*E-mail: masaya@tagen.tohoku.ac.jp. Tel.:+81-22-217-5637. Fax: +81-22-217-5642.

Notes

The authors declare no competing financial interest.

ACKNOWLEDGMENTS

We thank Prof. Keisuke Asai, Tohoku University, for the use of a pressure-controlled chamber. This work was supported by a Grant-in-aid for Scientific Research ((B) No. 24350112)) from the Japanese Society for the Promotion of Science (JSPS). The work was also supported by the Nano-Macro Materials, Devices and System Research Alliance (MEXT). M.M. thanks the Iketani Science and Technology Foundation for financial support.

REFERENCES

(1) Gennes, P.-G. de; Brochard-Wyart, F.; Quéré, D. Capillarity and Wetting Phenomena Drops, Bubbles, Pearls, Waves; Springer: New York, 2004.

(2) Deng, X.; Mammen, L.; Butt, H. J.; Vollmer, D. Candle Soot as a Template for a Transparent Robust Superamphiphobic Coating. *Science* **2012**, *335*, 67−70.

(3) Golovin, K.; Lee, D. H.; Mabry, J. M.; Tuteja, A. Transparent, Flexible, Superomniphobic Surfaces with Ultra-Low Contact Angle Hysteresis. *Angew. Chem., Int. Ed.* **2013**, *52*, 13007−13011.

(4) Bai, H.; Wang, L.; Ju, J.; Sun, R. Z.; Zheng, Y. M.; Jiang, L. Efficient Water Collection on Integrative Bioinspired Surfaces with Star-Shaped Wettability Patterns. *Adv. Mater.* **2014**, *26*, 5025−5030.

(5) Cassie, A. B. D.; Baxter, S. Wettability of Porous Surfaces. *Trans. Faraday Soc.* **1944**, *40*, 546−550.

(6) Shirtcliffe, N. J.; McHale, G.; Newton, M. I.; Perry, C. C.; Pyatt, F. B. Plastron Properties of a Superhydrophobic Surface. *Appl. Phys. Lett.* **2006**, *89*, 104−106.

(7) Chen, X.; Wu, Y. C.; Su, B.; Wang, J. M.; Song, Y. L.; Jiang, L. Terminating Marine Methane Bubbles by Superhydrophobic Sponges. *Adv. Mater.* **2012**, *24*, 5884−5889.

(8) Aebisher, D.; Bartusik, D.; Liu, Y.; Zhao, Y. Y.; Barahman, M.; Xu, Q. F.; Lyons, A. M.; Greer, A. Superhydrophobic Photosensitizers. Mechanistic Studies of O-1(2) Generation in the Plastron and Solid/Liquid Droplet Interface. *J. Am. Chem. Soc.* **2013**, *135*, 18990−18998.

(9) Amao, Y. Probes and Polymers for Optical Sensing of Oxygen. *Microchim. Acta* **2003**, *143*, 1−12.

(10) Lafuma, A.; Quere, D. Superhydrophobic states. *Nat. Mater.* **2003**, *2*, 457−460.

(11) Papkovsky, D. B.; Dmitriev, R. I. Biological Detection by Optical Oxygen Sensing. *Chem. Soc. Rev.* **2013**, *42*, 8700−8732.

(12) Borisov, S. M.; Wolfbeis, O. S. Optical Biosensors. *Chem. Rev.* **2008**, *108*, 423−461.

(13) Seddon, B. J.; Shao, Y.; Girault, H. H. Printed Microelectrode Array and Amperometric Sensor for Environmental Monitoring. *Electrochim. Acta* **1994**, *39*, 2377−2386.

(14) Ramamoorthy, R.; Dutta, P. K.; Akbar, S. A. Oxygen Sensors: Materials, Methods, Designs and Applications. *J. Mater. Sci.* **2003**, *38*, 4271−4282.

(15) Shin, I. S.; Hirsch, T.; Ehrl, B.; Jang, D. H.; Wolfbeis, O. S.; Hong, J. I. Efficient Fluorescence "Turn-On" Sensing of Dissolved Oxygen by Electrochemical Switching. *Anal. Chem.* **2012**, *84*, 9163−9168.

(16) Aminuzzaman, M.; Kado, Y.; Mitsuishi, M.; Miyashita, T. Preparation and Characterization of Poly(*N*-1H,1H-pentadecafluorooctylmethacrylamide) Langmuir−Blodgett Film. *Polym. J.* **2003**, *35*, 785−790.

(17) Matsukuma, D.; Watanabe, H.; Yamaguchi, H.; Takahara, A. Preparation of low-surface-energy poly[2−(perfluorooctyl)ethyl acrylate] microparticles and its application to liquid marble formation. *Langmuir* **2011**, *27*, 1269−1274.

(18) Nishino, T.; Meguro, M.; Nakamae, K.; Matsushita, M.; Ueda, Y. Preparation of Low-Surface-Energy Poly[2−(perfluorooctyl)ethyl acrylate] Microparticles and Its Application to Liquid Marble Formation. *Langmuir* **1999**, *15*, 4321−4323.

(19) Kim, Y.; Zhao, F.; Mitsuishi, M.; Watanabe, A.; Miyashita, T. Photoinduced High-quality Ultrathin SiO_2 Film from Hybrid Nanosheet at Room temperature. *J. Am. Chem. Soc.* **2008**, *130*, 11848−11849.

(20) Leezenberg, P. B.; Reiley, T. C.; Tyndall, G. W. Plasma Induced Copolymerization of Hexafluoropropylene and Octafluoropropane. *J. Vac. Sci. Technol., A* **1999**, *17*, 275−281.

(21) Mitsuishi, M.; Tanaka, H.; Obata, M.; Miyashita, T. Plasmon-Enhanced Luminescence from Ultrathin Hybrid Polymer Nanoassemblies for Microscopic Oxygen Sensor Application. *Langmuir* **2010**, *26*, 15117−15120.

(22) Wang, X. D.; Wolfbeis, O. S. Optical Methods for Sensing and Imaging Oxygen: Materials, Spectroscopies and Applications. *Chem. Soc. Rev.* **2014**, *43*, 3666−3761.

(23) Chu, C. S.; Lo, Y. L. Optical Fiber Dissolved Oxygen Sensor Based on Pt(II) Complex and Core−shell Silica Nanoparticles Incorporated with Sol−gel Matrix. *Sens. Actuators, B* **2010**, *151*, 83−89.

(24) Flynn, M. R.; Bush, J. W. M. Underwater Breathing: The Mechanics of Plastron Respiration. *J. Fluid Mech.* **2008**, *608*, 275−296.

(25) American Public Health Association, *Standard Methods for the Examination of Water and Wastewater: Including Bottom Sediments and Sludges*, 12th ed.; American Public Health Association: Washington, D.C., 1965.

(26) Moore, W. J. *Physical Chemistry*, fourth ed., Prentice Hall, Upper Saddle River, NJ, 1972.

DOI: 10.1021/am509147h
ACS Appl. Mater. Interfaces 2015, 7, 3468−3472